arXiv:1409.0613v1 [physics.atom-ph] 2 Sep 2014

On the symmetry of the electronic density in the three-electron parabolic quantum dot

A.V. Meremianin[1]

[1] *General Physics Department, Voronezh State University, 394006, Voronezh, Russia*

(Dated: September 3, 2014)

The structure of the lowest states of a three-electron axially symmetric parabolic quantum dot in a zero magnetic field is investigated. It is shown that the electronic density of the triplet states possesses certain approximate symmetry which is best seen when using Dalitz plots as the visualization tool. It is demonstrated that the origin of that symmetry is caused by the symmetry of the potential energy in the vicinity of its minimum. The discovered symmetry could provide an insight into the problem of the separation of slow and fast variables in the Schrodinger equation for the axially or spherically symmetric quantum dots.

PACS numbers: 03.65.Ge, 31.15.ae, 31.15.ve, 31.15.vj, 31.15xj, 73.21.La

I. INTRODUCTION

Quantum dots are semiconductor structures which can confine electrons. Therefore, they are often referred to as "artificial atoms". The theoretical study of few-electron quantum dots allows one to analyze the role of electronic correlations in nanostructures [1–3].

Often, a quantum dot can be modeled as a two-dimensional system of electrons having effective mass and confined via the axially symmetric parabolic potential. Quantum dots with one or two-electrons are comparatively simple to study since the corresponding theory can be developed using various analytical model approaches [3, 4]. Theoretical investigations of many-electron quantum dots are much more complicated because they require solution of many-dimensional partial differential equations which cannot be done analytically. Few-electron quantum dots are particularly difficult to study as in this case the application of various mean field approximations cannot be justified.

Obviously, the three-electron parabolic quantum dots are the simplest few-electron objects to analyze. They were studied rather extensively during the last decade [5–7]. In particular, much attention has been paid to the properties of the three-electron quantum dots in a magnetic field [8, 9]. In the mentioned papers the energy spectrum was calculated using various approaches and the structure of the electronic density was studied using pair-correlation functions. The latter, however, is not always appropriate as it could hide some interesting features of electronic density which are caused by triple correlations. In the three-body problem it is more instructive to analyze the structure of the electronic density directly, using some suitable set of internal variables. The treatment of the present article is based on the Dalitz-plot technique which is often used to analyze the angular distributions in three-body break-up processes in particle and molecular physics [10–13].

The use of Dalitz plots for the visualization of the electronic density greatly simplifies the analysis of its symmetries. Below it is shown that the Dalitz plots corresponding to the ground (and lowest excited) triplet states of the three-electron parabolic quantum dots posses some approximate symmetry similar to that observed in the model of the break-up of a three-body rigid rotator [14]. This symmetry means that, at a given value of the hyperradius which defines the overall "size" of the configuration triangle, the dependence of the electronic density on the area of that triangle is very much stronger than on its shape. The detailed analysis performed with the help of internal variables similar to "Dalitz-Fabri" coordinates [15, 16] explains the origin of the observed approximate symmetry (Sec. V). Namely, it is caused by the symmetry of the total potential in the vicinity of its local minimum. This symmetry can be uncovered by taking the power series expansion of the potential. For some particular values of the confinement strength the magnitude of the distortion of the symmetry is estimated in Sec. IV.

For the sake of brevity, numerical calculations were carried out only for states with zero angular momentum including the ground states of the quantum dot in the absence of external fields.

II. THE HAMILTONIAN OF THE THREE-ELECTRON QUANTUM DOT

The Schrödinger equation for the three electrons moving in a two-dimensional parabolic quantum dot is

$$-\frac{\hbar^2}{2m_e}\left(\sum_{i=1}^{3}\Delta_{\mathbf{R}_i}+U\right)\Psi_t = E\,\Psi_t, \tag{1}$$

$$U=\sum_{i=1}^{3}\frac{m_e\,\omega^2\,R_i^2}{2}+\sum_{i>j=1}^{3}\frac{e^2}{\epsilon\,|\mathbf{R}_i-\mathbf{R}_j|}, \tag{2}$$

where m_e is the effective electron mass and ϵ is the dielectric constant.

For the confinement potential given in Eq. (1) it is possible to separate out the motion of the c.m. of electrons by introducing two Jacobi vectors $\mathbf{r}_{1,2}$ as is shown in Fig. (1).

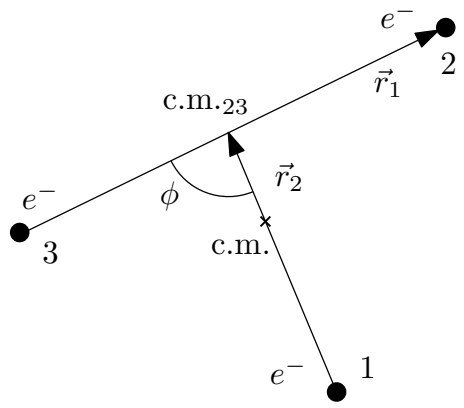

FIG. 1. Jacobi vectors for the three-body system. c.m$_{23}$ is the c.m. of the electrons 2 and 3.

The kinetic energy operator in terms of Jacobi vectors can be written as

$$-\sum_{i=1}^{3}\frac{\hbar^2}{2m_e}\frac{\partial^2}{\partial\mathbf{R}_i^2}=-\frac{\hbar^2}{6m_e}\frac{\partial^2}{\partial\mathbf{R}_{c.m.}^2}-\frac{\hbar^2}{m_e}\frac{\partial^2}{\partial\mathbf{r}_1^2}-\frac{3\,\hbar^2}{4m_e}\frac{\partial^2}{\partial\mathbf{r}_2^2}. \tag{3}$$

The sum of squared lengths of the position vectors rewritten via Jacobi vectors is diagonal,

$$R^2\equiv R_1^2+R_2^2+R_3^2=3R_{c.m.}^2+\frac{1}{2}r_1^2+\frac{2}{3}r_2^2. \tag{4}$$

It is convenient to introduce the mass-scaled Jacobi vectors by making the following replacements in Eqs. (3) and (4)

$$\mathbf{r}_1\to\sqrt{2}\,\mathbf{r}_1,\quad \mathbf{r}_2\to\sqrt{\frac{3}{2}}\,\mathbf{r}_2. \tag{5}$$

With these replacements the Schrödinger equation reads

$$(H_{c.m.}+H_{rel})\,\Psi_{tot}=E\,\Psi_{tot}, \tag{6}$$

where $H_{c.m.}$ is the Hamiltonian describing the motion of c.m. of three electrons,

$$H_{c.m.}=-\frac{\hbar^2}{6m_e}\frac{\partial^2}{\partial\mathbf{R}_c^2}+\frac{3m_e\,\omega^2\,R_{c.m.}^2}{2}, \tag{7}$$

and H_{3e} is the Hamiltonian corresponding to the internal (relative) motion of electrons in the parabolic trap

$$H_{rel}=-\frac{\hbar^2}{2m_e}\,(\Delta_1+\Delta_2)+\frac{m_e\,\omega^2\,(r_1^2+r_2^2)}{2}+e^2\kappa\,U_{cl}, \tag{8}$$

where $\Delta_{1,2}=\partial^2/\partial\mathbf{r}_{1,2}^2$, $\kappa=1/\epsilon$ and U_{cl} denotes the Coulomb repulsion terms

$$U_{cl}=\frac{1}{\sqrt{2}\,r_1}+\frac{\sqrt{2}}{|\mathbf{r}_1+\mathbf{r}_2\sqrt{3}|}+\frac{\sqrt{2}}{|\mathbf{r}_1-\mathbf{r}_2\sqrt{3}|}. \tag{9}$$

Dividing the Schrödinger equation by $\hbar\omega$ it can be brought to dimensionless form by making the replacements $r_{1,2}\to r_{1,2}\sqrt{\hbar/(m_e\omega)}$. As a result, the Hamiltonian assumes the form

$$H_{rel}=-\frac{\Delta_1+\Delta_2}{2}+\frac{r_1^2+r_2^2}{2}+R_c\,U_{cl}, \tag{10}$$

where the variables $r_{1,2}$ are dimensionless and R_c is the Coulomb strength parameter,

$$R_c=\frac{e^2\kappa}{\hbar}\sqrt{\frac{m_e}{\hbar\omega}}=\alpha\kappa\sqrt{\frac{m_ec^2}{\hbar\omega}}, \tag{11}$$

where α is the fine structure constant. The numerical calculations were carried out with the effective electron mass $m_e=0.067m$ and $\kappa=12.4$, which correspond to GaAs, so that

$$R_c=\frac{3.443}{\sqrt{(\hbar\omega)_{\rm mEv}}}. \tag{12}$$

III. DALITZ PLOTS OF THE ELECTRONIC DENSITY

The electronic density $D_n(\xi)=|\Psi_n(\xi)|^2$ in the three-electron quantum dot depends on three internal variables $\xi=(\xi_1,\xi_2,\xi_3)$. Thus, $D_n(\xi)$ is a surface in the four-dimensional space and as such cannot be visualized. However, if we fix one of the internal variables, say ξ_1, then the function $D_n(\xi_1=const,\xi_2,\xi_3)$ becomes a three-dimensional surface which can be depicted on a sheet of paper as a color intensity map. Since the hyperradius R is independent of the particle exchange, it is convenient to visualize $D_n(\xi)$ as a series of 3d surfaces with variable values of $R=0,\ldots,R_{max}$. Now the question is how to choose the two remaining internal variables to facilitate the features of the electronic density. Below we will use the two dimensionless internal coordinates similar to those of a Dalitz plot which was initially proposed to visualize the angular distributions of K mesons in particle physics [10].

Conventional Dalitz plots are the diagrams which depict the angular distributions of linear momenta of three particles [10, 11]. The feature of the Dalitz plot is that each configuration of particle's momenta is represented as a point inside a circle so that the exchange of particles is equivalent to the rotation by the angle $(2/3)\pi$ with respect to the center of the plot which itself corresponds to the equilateral configuration when vectors of particle's momenta form an equal-side triangle. Points on the edge of the circle describe collinear configurations when particles fly apart along the same line.

To apply the Dalitz plot technique to the analysis of the electronic density we choose the coordinates of the polar plot to be the Dalitz coordinates [10, 17] in 2d configuration space

$$x=\frac{R_1^2-R_2^2}{\sqrt{3}\,R^2},\quad y=\frac{1}{3}-\frac{R_3^2}{R^2}. \tag{13}$$

Here, it is assumed that CM of the three electrons is located at the origin of the coordinate frame, i.e.

$$\mathbf{R}_{c.m.} = \mathbf{R}_1 + \mathbf{R}_2 + \mathbf{R}_3 = 0. \tag{14}$$

The Dalitz coordinates (13) can also be expressed in terms of mass-scaled Jacobi vectors as

$$\begin{aligned} x &= \frac{1}{2\sqrt{3}\,R^2}\left(r_2^2 - r_1^2 - \frac{1}{\sqrt{3}}(\mathbf{r}_1\cdot\mathbf{r}_2)\right), \\ y &= \frac{1}{6\,R^2}\left(r_2^2 - r_1^2 + 2\sqrt{3}(\mathbf{r}_1\cdot\mathbf{r}_2)\right), \end{aligned} \tag{15}$$

where the hyperradius $R = r_1^2 + r_2^2$.

In literature are often used the symmetry adapted hyperspherical coordinates also known as "Dalitz-Fabri coordinates" [15, 16, 18, 19] which are defined by

$$\begin{aligned} r_2^2 - r_1^2 &= R^2 \sin a\, \cos\lambda, \\ (\mathbf{r}_1\cdot\mathbf{r}_2) &= \frac{R^2}{2}\sin a\, \sin\lambda. \end{aligned} \tag{16}$$

where $0 \le a \le \pi/2$ and $0 \le \lambda \le 2\pi$.

Note that the hyperangles a, λ were, in fact, originally introduced by Gronwall and published in his posthumous paper [18] where the Hamiltonian of the Helium atom [18] was written in terms of the variables R, a, λ. Therefore, below these coordinates will be referred to as Gronwall-Dalitz-Fabri (GDF) coordinates.

Coordinates having similar kinematical properties as GDF coordinates (16) were used in molecular physics by several authors including Kuppermann [20], Mead [21], Pack [22]. Mishra and Linderberg [23] used Mead coordinates to visualize potential energy surfaces in triatomic molecules.

From Eqs. (15), (16) one can deduce the connection of Cartesian coordinates x, y to hyperangles a, λ,

$$\begin{aligned} x &= \frac{\sin\alpha}{3}\,\cos\left(\lambda + \frac{\pi}{6}\right), \\ y &= \frac{\sin\alpha}{3}\,\sin\left(\lambda + \frac{\pi}{6}\right), \end{aligned} \tag{17}$$

From these equations it follows that the polar radius ρ on the Dalitz plot is

$$\rho \equiv \sqrt{x^2 + y^2} = \frac{\sin a}{3}. \tag{18}$$

Noting the identity (4) one obtains immediately that

$$\rho^2 = \frac{1}{9} - \frac{4\,|\mathbf{R}_1 \times \mathbf{R}_2|^2}{3R^4}. \tag{19}$$

From Eqs. (19) and (14) it is seen that the polar radius ρ of the Dalitz plot is invariant under the particle exchange. This means that the exchange of particles is equivalent to the rotation or reflection of the diagram.

Note also that in terms of Jacobi vectors expression (19) reads

$$\rho^2 = \frac{1}{9} - \frac{4\,|\mathbf{r}_1 \times \mathbf{r}_2|^2}{27R^4}. \tag{20}$$

Positions of particles define the vertices of the triangle (i.e. the configuration triangle) whose area is

$$S = \frac{1}{2}|\mathbf{r}_1 \times \mathbf{r}_2|. \tag{21}$$

Thus, Eq. (20) means that the square polar radius of the Dalitz plot is proportional to the area of the configuration triangle,

$$\rho^2 = \frac{1}{9} - \frac{16\,S^2}{27R^4}. \tag{22}$$

IV. THE NUMERICAL RESULTS

The wave function of the three electrons was obtained by diagonalizing the Hamiltonian (10) in the basis of Fock-Darwin states [24, 25] which are defined by

$$\Psi_{n,m}(\mathbf{r}) = \frac{e^{-im\phi}}{\sqrt{2\pi}}\,\psi_{n,m}(r), \tag{23}$$

$$\begin{aligned} \psi_{n,m}(r) = &\sqrt{\frac{n!}{(n+|m|)!}}\left(\frac{r}{\sqrt{2}}\right)^{|m|} \\ &\times e^{-r^2/4} L_n^{|m|}\left(\frac{r^2}{2}\right), \end{aligned} \tag{24}$$

where $L_n^{|m|}$ is the associated Laguerre polynomial [26]. Fock-Darwin wave functions (23) diagonalize the Hamiltonian of an electron in a parabolic circular trap. The corresponding single-electron energy is (in units of $\hbar\omega$)

$$E_{n,m} = (2n + 1 + |m|). \tag{25}$$

The wave function of an S-state can be expanded over the Fock-Darwin states as

$$\Psi(\mathbf{r}_1, \mathbf{r}_2) = \sum_{n=0}^{N}\sum_{n'=0}^{N}\sum_{m=-m_0}^{m_0} F_{nn',m}\,\Psi_{n,m}(\mathbf{r}_1)\,\Psi_{n',-m}(\mathbf{r}_2), \tag{26}$$

where N and m_0 determine the accuracy of the representation of the wave function. The number of terms in the expansion Eq. (26) is

$$Z_{Nm_0} = (N+1)^2\,(2m_0 + 1). \tag{27}$$

The satisfactory convergence was achieved at $N, m_0 \sim 5 - 7$. Obtained results for the energy of the ground states are in good agreement with existing in literature [27]. Note that large values of N, m_0 lead to occurrence of spurious oscillations which degrades the accuracy of computations [28].

Dalitz plots of the ground state electronic density $D_0 = |\Psi_0(R, a, \lambda)|^2$ are given in Fig. 2 for the Coulomb strength parameter $R_c = 5.444$ (which corresponds to the confinement energy $\hbar\omega = 0.40$ mEv) and two values of the hyperradius R. As is seen, the density has maximum at the center of the plot which is the equilateral

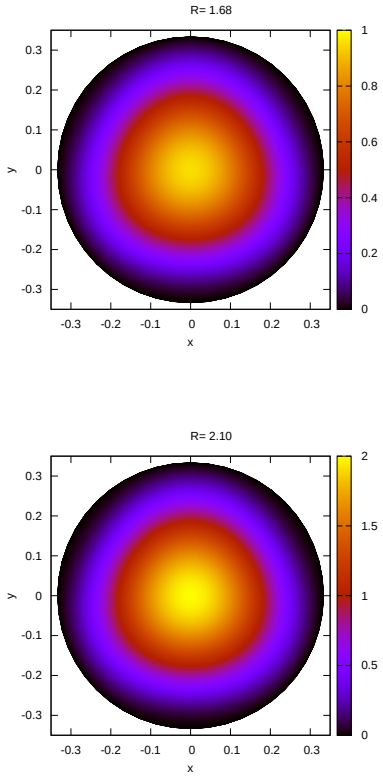

FIG. 2. (Color online) The Dalitz plot for the electronic density of the ground state at the confinement energy $\hbar\omega = 0.40$ mEv ($R_c = 5.444$) for two values of hyperradius R.

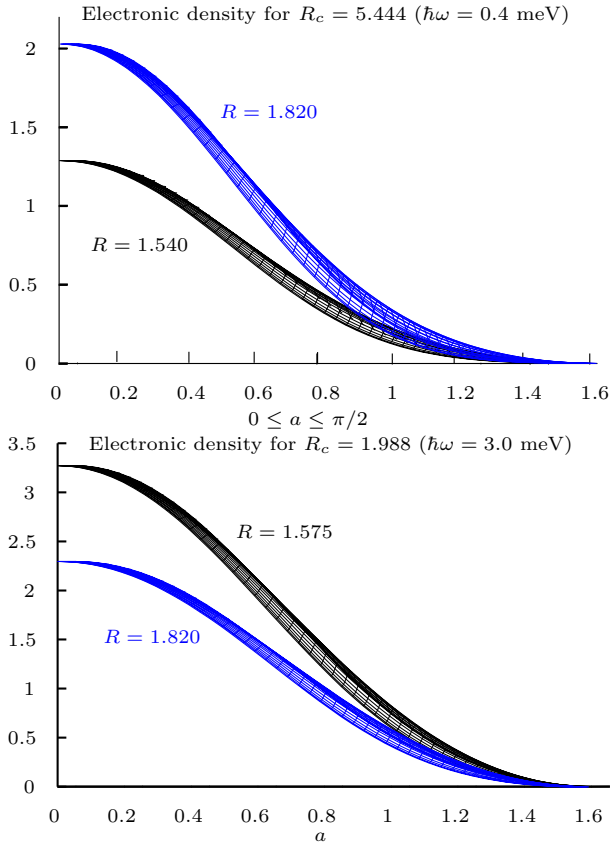
Electronic density for $R_c = 5.444$ ($\hbar\omega = 0.4$ meV)
$R = 1.820$
$R = 1.540$
$0 \le a \le \pi/2$
Electronic density for $R_c = 1.988$ ($\hbar\omega = 3.0$ meV)
$R = 1.575$
$R = 1.820$
a

FIG. 3. (Color online) Projections of the electronic density $D_0 = |\Psi_0(R, a, \lambda)|^2$ of the ground S-state on the plane $\lambda = const$ for two values of the Coulomb strength parameter R_c. Note that in the case of independence of the density on the hyperangle λ the projections would be single thin lines.

configuration and decreases as the configuration triangle becomes more prolate, finally vanishing for collinear configurations.

The striking feature of the diagrams in Fig. 2 is the remarkably weak dependence of the density on the polar angle of the plot. In order to estimate the magnitude of this dependence, Fig. 3 shows the projection of the density $D_0(R, a, \lambda)$ on the surface $\lambda = const$ of the Cartesian frame with coordinates $(x_1, x_2, x_3) = (a, \lambda, D_0)$. Note that the width of the curves shown in Fig. 3 is determined by the variation of the density as a function of the polar angle (which is actually $\lambda+\pi/6$, see Eqs. (17)). The structure of the electronic density shown in Figs. 2,3 is preserved also for other values of the hyperradius R, [29], [30]. The Dalitz plots corresponding to the excited triplet states also have circular symmetry similar to that shown in Fig. 2. However, the computations of the wave functions for the excited states are less accurate than those of the eigenvalues and the corresponding results are not shown here.

V. ON THE ORIGIN OF THE SYMMETRY

In terms of position vectors the potential energy of the electron-electron interaction in the quantum dot reads ($e = 1$)

$$U = \frac{1}{R_{12}} + \frac{1}{R_{23}} + \frac{1}{R_{31}}, \tag{28}$$

where $R_{ij} = \mathbf{R}_i - \mathbf{R}_j$.

According to Earnshaw's theorem, the potential energy of the system of particles interacting via Coulomb forces cannot have minimum. However, in the case of electrons in a parabolic trap the equilibrium configurations can exist, i.e. there are minima of the *total* potential energy. Thus, it is possible to expand the potential (28) in the vicinity of the equilibrium configuration. For example,

the expansion of the first term in Eq. (28) has the form

$$\frac{1}{R_{12}} = \sum_{k=0}^{\infty} \frac{1}{k!}((\mathbf{R}_{12} - \mathbf{R}_{12}^{(e)}) \cdot \nabla)^k \, \frac{1}{r}\Big|_{r=R_{12}^{(e)}} = \\ = \frac{1}{R_{12}^{(e)}} + \left(\frac{1}{R_{12}^{(e)}} - \frac{(\mathbf{R}_{12} \cdot \mathbf{R}_{12}^{(e)})}{{R_{12}^{(e)}}^3}\right) \\ + \left(\frac{1}{R_{12}^{(e)}} - \frac{R_{12}^2 + 4(\mathbf{R}_{12} \cdot \mathbf{R}_{12}^{(e)})}{2{R_{12}^{(e)}}^3} + 3\frac{(\mathbf{R}_{12} \cdot \mathbf{R}_{12}^{(e)})^2}{2{R_{12}^{(e)}}^5}\right) + \ldots, \tag{29}$$

where $\mathbf{R}_{ij}^{(e)}$ is the position vector pointing from i-th to j-th electron at the equilibrium configuration. For the equilibrium configuration being an equilateral triangle we have that $R_{12}^{(e)} = R_{23}^{(e)} = R_{31}^{(e)} \equiv R_e$. If we restrict ourselves only to zero- and first-order terms in the expansion (29) then the Coulomb potential (28) becomes

$$U = \frac{6}{R_e} - \frac{(\mathbf{R}_{12} \cdot \mathbf{R}_{12}^{(e)}) + (\mathbf{R}_{23} \cdot \mathbf{R}_{23}^{(e)}) + (\mathbf{R}_{31} \cdot \mathbf{R}_{31}^{(e)})}{R_e^3}. \tag{30}$$

We have to specify also the mutual orientation of the two configuration triangles, one built on equilibrium mutual vectors $\mathbf{R}_{12}^{(e)}, \mathbf{R}_{23}^{(e)}, \mathbf{R}_{31}^{(e)b}$ and another one built on the instantaneous vectors $\mathbf{R}_{12}, \mathbf{R}_{23}, \mathbf{R}_{31}$. This can be done by using the moving frame which satisfies the Eckart condition [31]

$$[\mathbf{R}_{12}^{(e)} \times \mathbf{R}_{12}] + [\mathbf{R}_{23}^{(e)} \times \mathbf{R}_{23}] + [\mathbf{R}_{31}^{(e)} \times \mathbf{R}_{31}] = 0. \tag{31}$$

In terms of mass-scaled Jacobi vectors this equality reads

$$[\boldsymbol{\rho}_1 \times \mathbf{r}_1] + [\boldsymbol{\rho}_2 \times \mathbf{r}_2] = 0. \tag{32}$$

where $\boldsymbol{\rho}_{1,2}$ are the equilibrium mass-scaled Jacobi vectors. As a result, the potential energy (30) assumes the form

$$U = \frac{6}{R_e} - 3\,\frac{(\boldsymbol{\rho}_1 \cdot \mathbf{r}_1) + (\boldsymbol{\rho}_2 \cdot \mathbf{r}_2)}{R_e^3}. \tag{33}$$

In the Eckart frame defined by Eq. (32) the sum $(\boldsymbol{\rho}_1 \cdot \mathbf{r}_1) + (\boldsymbol{\rho}_2 \cdot \mathbf{r}_2)$ defines the Eckart parameter $\mathcal{F}$ which can be written as [32, 33]

$$\mathcal{F} = \sqrt{(\rho_1 r_1)^2 + (\rho_2 r_2)^2 + 2\rho_1\rho_2 r_1 r_2 \, \cos(\phi - \phi_e)}, \tag{34}$$

where ϕ_e is the angle between vectors $\boldsymbol{\rho}_1$ and $\boldsymbol{\rho}_2$. For the equilibrium configuration being an equilateral triangle we have that $\phi_e = \pi/2$ and $\rho_1 = \rho_2 = R_e/\sqrt{2}$ and the above identity becomes

$$\mathcal{F} = R_e\sqrt{(r_1^2 + r_2^2)/2 + r_1 r_2 \, \sin\phi]}. \tag{35}$$

In terms of GDF variables the Eckart parameter assumes rather simple form

$$\mathcal{F} = \frac{R_e R}{2}\sqrt{2 + 3\cos^2 a}. \tag{36}$$

Consequently, the potential energy (33) evaluates to

$$U = \frac{3}{2R_e}\left(4 - \frac{R}{R_e}\sqrt{2 + 3\cos^2 a}\right). \tag{37}$$

As is seen, the potential energy does not depend on the second hyperangle λ and, hence, the dependence of the wave function on λ is caused by the contribution of higher order terms in the expansion of the Coulomb potential (29). The numerical calculations presented above allows one to estimate the contribution of the higher-order multipoles in the expansion of Coulomb terms to be less than 10% for the chosen values of the electron effective mass and the confinement strength.

VI. CONCLUSION

In the presented article the symmetry of the electronic density of the circular parabolic three-electron quantum dots has been investigated. It is found that the electronic density (and the wave functions) of the triplet states depends on the shape of the configuration triangle much weaker than on its overall size and area. Such property of the density can be understood by employing the power (i.e. multipole) expansion of the total potential energy around the equilibrium configuration. The mentioned symmetry is best seen in the Dalitz diagrams for the electronic density (Sec. III). The Dalitz diagrams suggest that the internal variables most suited for the description of the problem are the Gronwall-Dalitz-Fabri coordinates R, a, λ (see Eq. (16) of Sec. III) because among these coordinates the hyperangle λ is the "slow variable" as it describes the shape of the configuration triangle.

Note that the approach employed above to explain the origin of the symmetry (Sec. V) was not limited to the case of planar quantum dots for which the numerical results were presented in Sec. IV. Thus, one can expect that some approximate symmetries similar to that uncovered in this article will show up in the three-dimensional case when three electrons are confined by an arbitrary spherically symmetric potential. Further, the consideration given in Sec. V can be easily generalized to the case of four- and more electrons which gives the possibility to distinguish slow and fast variables in the corresponding wave functions. This, however, needs more detailed investigations.

Another interesting problem would be to analyze the influence of an external magnetic field on the symmetry of the electronic density. For example, the application of the transversal magnetic field to a planar quantum dot does not violate the circular symmetry of the Hamiltonian and, therefore, should not change the symmetry drastically. However, if the magnetic field has components parallel to the plane of the quantum dot, then the symmetry of the electronic density will be broken. Again, this is the subject of further research. Note that effects of symmetry breaking in finite systems were recently reviewed in Ref. [34].

ACKNOWLEDGMENTS

This work has been supported in part by the Ministry of Education and Science of Russia (Project No 1306).

[1] C. G. Bao, Phys. Rev. Lett. **79**, 3475 (1997).

[2] P. A. Macsym, H. Imamura, G. P. Mallon, and H. Aoki, J. Phys. Condens. Matter **12**, R299 (2000).

[3] A. Puente, L. Serra, and R. G. Nazmitdinov, Phys. Rev. B (Condensed Matter and Materials Physics) **69**, 125315 (pages 9) (2004), URL http://link.aps.org/abstract/PRB/v69/e125315.

[4] N. S. Simonovic and R. G. Nazmitdinov, Phys. Rev. B **67**, 041305 (2004).

[5] R. Egger, W. Häusler, C. H. Mak, and H. Grabert, Phys. Rev. Lett. **82**, 3320 (1999), URL http://link.aps.org/doi/10.1103/PhysRevLett.82.3320.

[6] S. A. Mikhailov, Phys. Rev. B **65**, 115312 (2002).

[7] N. S. Simonovic, Few-Body Systems **38**, 139 (2006).

[8] M. Taut, Journal of Physics: Condensed Matter **21**, 075302 (2009), URL http://stacks.iop.org/0953-8984/21/i=7/a=075302.

[9] A. Fang, X. Chi, and P. Sheng, Solid State Communications **142**, 551 (2007), ISSN 0038-1098,

[10] R. H. Dalitz, Philos. Mag **44**, 1068 (1953).

[11] U. Müller, T. Eckert, M. Braun, and H. Helm, Phys. Rev. Lett. **83**, 2718 (1999).

[12] U. Galster, F. Baumgartner, U. Müller, H. Helm, and M. Jungen, Phys. Rev. A **72**, 062506 (2005).

[13] J. D. Savee, V. A. Mozhayskiy, J. E. Mann, A. I. Krylov, and R. E. Continetti, Science Magazine **321**, 826 (2008), URL http://dx.doi.org/10.1126/science.1157617.

[14] A. V. Meremianin, Few-body Systems **38**, 199 (2006).

[15] V. D. Efros, A. M. Frolov, and M. I. Mukhtarova, J. Phys. B: At. Mol. Phys. **15**, L819 (1982), URL http://stacks.iop.org/0022-3700/15/i=23/a=001.

[16] R. Krivec, Few-Body Systems **25**, 199 (1998).

[17] E. Fabri, Il Nuovo Cimento (1943-1954) **11**, 479 (1954), ISSN 1827-6121, 10.1007/BF02781042, URL http://dx.doi.org/10.1007/BF02781042.

[18] T. H. Gronwall, Phys. Rev. **51**, 655 (1937), URL http://link.aps.org/doi/10.1103/PhysRev.51.655.

[19] A. Badalyan and Y. Simonov, Yadern. Fiz. **3**, 1032 (1966).

[20] A. Kuppermann, Chem. Phys. Lett. **32**, 374 (1975), ISSN 0009-2614,

[21] C. A. Mead, Rev. Mod. Phys. **64**, 51 (1992).

[22] R. T Pack, Chem. Phys. Lett. **230**, 223 (1991).

[23] M. Mishra and J. Linderberg, Mol. Phys. **50**, 91 (1983).

[24] C. G. Darwin, Proc. Camb. Phil. Soc. **27**, 86 (1930).

[25] V. A. Fock, Z. Phys. **47**, 446 (1928).

[26] A. Erdelyi, W. Magnus, F. Oberhettinger, and F. G. Tricomi, *Higher trancendental functions. Bateman manuscript project*, vol. II (McGraw-hill book company, Inc, 1953).

[27] X. Wen-Fang, Communications in Theoretical Physics **48**, 1115 (2007), URL http://stacks.iop.org/0253-6102/48/i=6/a=030.

[28] M. Haftel and V. Mandelzweig, Annals of Physics **189**, 29 (1989).

[29] Supplementary material. Motion picture of the Dalitz plots of the ground state electronic density for $\hbar\omega = 0.40$ mEv and the hyperradius $R = 0, \ldots, 3.4$. URL To be inserted by publisher Dalitz_0_40.avi

[30] Supplementary material. The ground state electronic density for $\hbar\omega = 0.40$ mEv and the hyperradius $R = 0, \ldots, 3.4$ as a series of pictures similar to Fig. 3. URL To be inserted by publisher Density_0_40.avi

[31] C. Eckart, Phys. Rev. **47**, 552 (1935).

[32] A. V. Meremianin, J. Chem. Phys. **120**, 7861 (2004).

[33] A. Meremianin, J. Math. Chem. **51**, 1376 (2013), ISSN 0259-9791, URL http://dx.doi.org/10.1007/s10910-013-0152-9.

[34] J. L. Birman, R. G. Nazmitdinov, and V. Yukalov, Phys. Rep. **526**, 1 (2013), URL http://dx.doi.org/10.1016/j.physrep.2012.11.005.